Available online at www.sciencedirect.com

ScienceDirect

Physics Procedia 56 (2014) 1115 – 1125

Physics Procedia

8th International Conference on Photonic Technologies LANE 2014

Laser nanostructuring of the PbX thin films for creation of the semiconductor devices with controlled properties

S.M. Arakelian[a], D.N. Bukharov[a], V.I. Emel'yanov[b], S.P. Zimin[c], S.V. Kutrovskaya[a], A.O. Kucherik[a,*], A.A. Makarov[a], A.V. Osipov[a]

[a]*Vladimir State University named after Alexander and Nikolay Stoletovs, Vladimir, Gorky str., 87, 600000, Russian Federation*
[b]*Lomonosov Moscow State University, Moscow, Leninskie Gory, 119991, Russian Federation*
[c]*P.G. Demidov Yaroslavl State University, Yaroslavl, Sovetskaya str., 10, 150000, Russian Federation*

Abstract

We have studied a solid-state laser modification of the surface of PbX semiconductor films under processes of self-organization for conditions when photon energies are above the band gap of the semiconductor. Experimental data were used to construct a model for defect deformation instability developing on the surface of epitaxial film through strain-induced drift of laser-induced point defects. The model is capable to describe qualitatively observed surface morphology and to predict the surface profile in laser modification experiments.

It has been demonstrated that used approach is applied to analyze ant structure with various morphology which depends on parameters of laser action. By changing the electro-physical properties of the created structures in necessary direction we have a good opportunity to fabricate the new devices for optoelectronics and photonics of different kind.

Peer-review under responsibility of the Bayerisches Laserzentrum GmbH

Keywords: laser treatment; nanostructuring; solid-state modification; DD-theory

* Corresponding author. Tel.: +7-89157617615 .
E-mail address: kucherik@vlsu.ru

Peer-review under responsibility of the Bayerisches Laserzentrum GmbH
doi:10.1016/j.phpro.2014.08.026

1. Introduction

The laser irradiation of the semiconductor surface results in many opportunities to the nanoparticle synthesis. The method allows to control a lateral size, density distribution and size distribution. The interest in these structures caused by changes in their optical and electrical properties compared to bulk samples due to dimensional effects [1-3]. The properties variation of nanostructured materials is very well known for colloidal systems, when the changing of the particle size results in dramatic modification of physic-chemical states e.g. in mechanical properties shift of the absorption and luminescence [4-5], due to surface topology modification for semiconductor materials [6-9], etc. in comparison with the base material.

Short (ns) and ultrashort (fs) laser pulse durations which result in surface melting and ablation [4,6-9] are usually used for nanostructuring materials [7]. However, the possibility of the solid semiconductor surfaces (lead chalcogenides PbTe, PbSe) nanostructuring by continuous laser radiation has been shown in our previous studies [10-12]. The last case is very perspective in two aspects. First, in fundamental meaning because the equilibrium phase transitions occur by controlled way. Second, in applied respect due to the formation of nanoparticles/nanoclusters with controlled both size and topology distribution on the surface of a thin film. The fact allows to create the gradient materials with varying properties depending on the morphology. In fact, when lateral sizes of obtained nanostructures are substantially greater than their height, the property difference occurs in comparison with the spherical particles with the same composition (see [12]). E.g. when the lateral size of the particles is in the range 100-300 nm, but their height is about 30-60 nm, the energy levels shift and bandgap can be observed in the perpendicular direction to the substrate surface in contrast to the effects in the substrate plane, being expressed weaker. It can be expected that in the spatial distribution of such regularly spaced particles on the surface, the effects of long and short range order should be observed and the problem of quasiparticles development on the semiconductor surface.

Earlier [11] we have proposed the method of forming the nanoparticle ensemble using the continuous laser radiation acting on lead telluride (PbTe) film. The material is perspective due to the narrow semiconductor bandgap equal 0.32 eV (300 K); the exciton Bohr radius for this case is up to 150 nm [13]. That is why it can be used to solve different problems of photonics and electronics to create devices with variable optical and electrical properties. In this paper we will discuss the new results in the field for epitaxial films of PbTe under cw-laser radiation.

2. Experiment

The original heteroepitaxial structures PbTe/CaF_2/Si (111) were grown by the molecular beam epitaxy in the laboratory ETH (Zurich). Film thicknesses were ranged from 1 to 6 microns, a buffer layer CaF_2 (thickness – 2-4 nm) was deposited for difference compensation of the silicon substrate lattice constants and an epitaxial film. The features of the lead telluride film layering and the parameters of studied films are described in detail in [14]. PbTe layers had a single crystal structure with (111) orientation along the growth axis. The film surface had a block structure with a lateral size of blocks 1-3 microns and the height difference was 10-20 nm (Fig. 1).

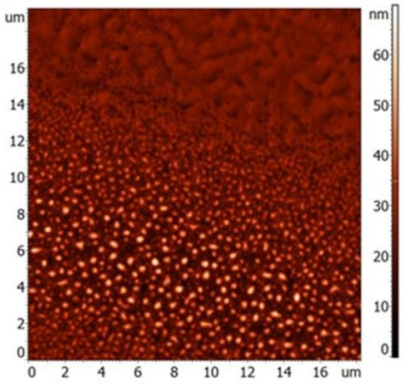

Fig. 1. AFM-image of the PbTe surface after 7 W laser treatment, laser beam diameter – 50 μm. The ensemble of nanoparticles formed within the

irradiation area is in the lower left corner. In the upper right corner – the image for original surface of the film.

The experimental setup of [11,12] has been used for laser irradiation of the samples. The YAG:Nd (λ = 1.06 μm) laser radiation of 6-10 W, focused on the sample surface into 30-100 μm as a beam diameter. The exposure intensity was 10^5-10^6 W/cm^2 (Gaussian profile distribution). The sample scanning under laser irradiation has been performed on the stepwise coordinate table (40-160 μm/s). The laser heating control of the surface in a real time has been realized using the original diagnostic system «laser monitor» described in [12].

3. The film surface modification under laser irradiation

The formed ensemble of PbTe-nanoparticles in the laser beam spot size had a bimodal distribution function in respect of lateral size d (Fig. 2), which has two clearly expressed peaks. The first peak was narrow width maximum for d = 100 nm, the second peak was broader and located at d = 300 nm.

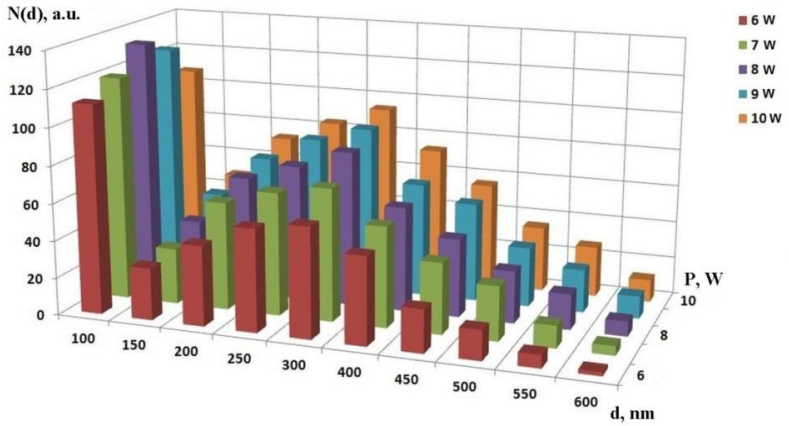

Fig. 2. Histograms of the particles distribution in the laser action area. The thickness of the column is ±10 nm relatively to the average size. Laser beam diameter is 30 microns, the scanning speed is 80 m/s.

The effect of formation of nanoparticles with a bimodal distribution is observed in a narrow range of power (6-10W) for the beam diameter of 30-100 microns and without film thickness dependence. The most intense formation of particles on the surface has been observed with a scanning speed of 80 μm/s for laser beam. The radiation power variation in the range 6-10 W, first slightly changes the amplitude of two peaks, but second, does not changes the principle parameters – position and width (Fig. 2) of the peaks. The increasing of intensity of laser radiation results in linear increasing of the quantity of particles N formed in the surface modification area with the tendency to the nonlinear behavior (Fig. 3).

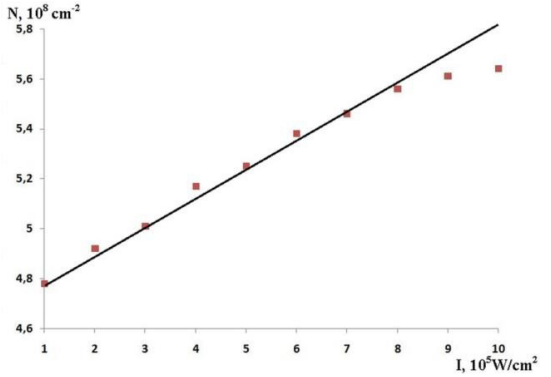

Fig. 3. The quantity of nanoparticles N under laser modification of the surface vs laser intensity I: points - experiment; solid line - approximation.

4. The simulation of the laser heating process for a thin epitaxial PbTe

We discuss now the analysis results of the temperature field when the target surface is scanned by laser radiation. Because of the thermal diffusion length (~ 1 mm), being perpendicular to the surface during the scanning of the laser beam is much larger than the absorption length (~ 1 μm)of the laser radiation, the heat source can be considered as superficial. Then, the heating surface model process has been implemented using the Matlab library functions with MatlabLaserToolbox [15].

The distribution intensity of the laser radiation can be presented as a Gaussian like beam on the plane XY of irradiated surface:

$$I(x,y)=\frac{8P}{\pi d^2}\exp\left[-\left(\frac{2\sqrt{2}}{d}\right)^2\left(x^2+y^2\right)\right], \tag{1}$$

where P – laser power, d – diameter of the beam on the target surface.

The temperature field of a moving surface source is:

$$T(x,y,z,t)=\int_{-\infty}^{\infty}\!\!\int AI(x',y')W(x,y,z,x',y',\upsilon)\,dx'dy', \tag{2}$$

where $W(x,y,z,x',y',\upsilon)=\frac{1}{2\pi KR}\exp(-\frac{\upsilon}{2a}(x-x'+R)$ and $R=\sqrt{x^2+y^2+z^2}$,

where K – thermal conductivity (W/m*K), $a=K/\rho c_p$ – thermal diffusivity (m^2/s) of the material, A – absorbance of the material, υ – scanning speed, ρ – density of bulk material, c_p – heat capacity.

The system of equations (1) – (2) has been solved using the fast Fourier transform (FFT) [15]. According to the proposed model, The results of calculations for the temperature field distribution on the target surface) in a square area of 400 microns for lead telluride (A = 0.3, ρ = 8200 kg/m^3, c_p = 151 J/kg*K, K = 2.3 W/m*K), and the laser radiation parameters (power in the center of the area P = 8 W, a laser beam diameter d = 30 μm and d = 100 μm for a scan rate of 80 m/s) are shown in Fig. 4. Starting plate temperature for the sample is 300 K.

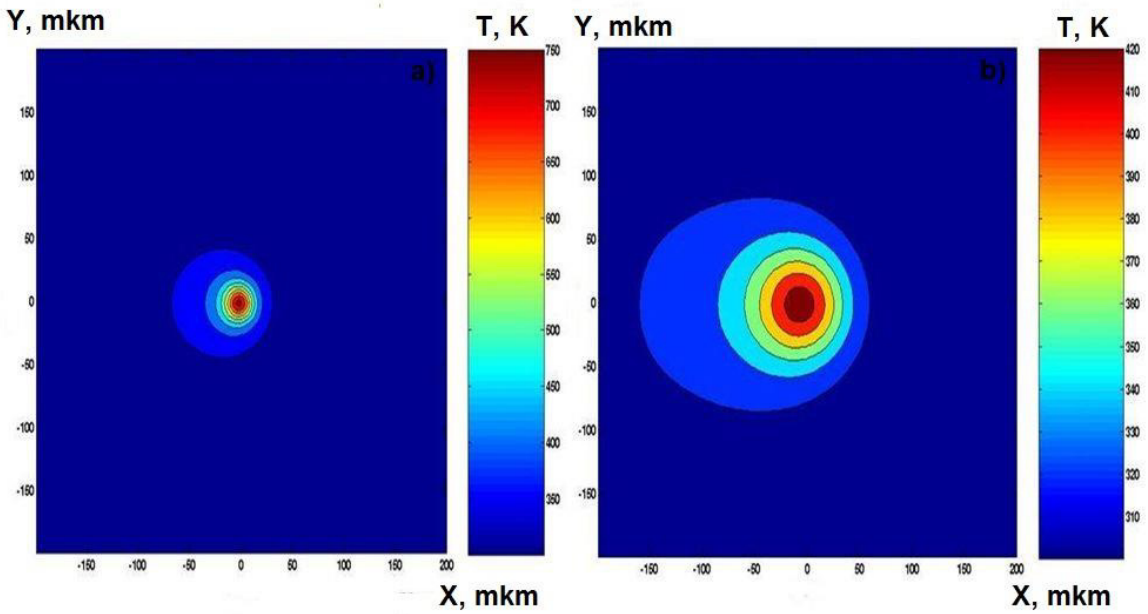

Fig. 4. Temperature field on the PbTe film (plane z = 0): the laser beam scanning velocit over the surface – v = 80 μm/s, laser power P = 8 W, the laser beam diameter = 30 μm (a) and d = 100 μm (b).

Fig. 4 shows that in the case of the laser spot diameter of 30 μm the maximum temperature occurs in the center of the spot and has a value 776 ^{O}K. The figure is lower than the lead telluride melting temperature (1190 ^{O}K). For increasing of the laser beam diameter the temperature field expands considerably as well, but the value of temperature is significantly lower, i.e. 420 ^{O}K in the center of the spot. The temperature distribution is asymmetric on the surface plane and elongated in the direction of scan. There is a feature of the heating by the moving source: the material in front of it $(x > 0)$ warms slightly; warming area is about the diameter of the laser beam; the moving source leaves weakly damped temperature loop about a quarter of the length of the warming field behind it. In the center of the laser spot the temperature had reached 771 ^{O}K during the time of 1 s increased gradually to a maximum 776 ^{O}K. Because this temperature is significantly below the melting point of lead telluride, it is possible to assert that the solid-phase modification occurs in the laser heating field.

5. The defect-deformation theory of the formation of bimodal nanoparticle ensembles under cw-laser irradiation of solids

The defect-deformation theory for modeling of the experiments which took part in this paper we discussed in the earlier paper [16]. Here we particularly repeat the main ideas of the DD-theory with the addition of the results for description of new experiments. The absorption of incident laser radiation in semiconductor (absorption length, labs) produces a plasma-enriched surface layer, whose thickness is equal to the carrier diffusion length $l_{dif} = \left(D_e \tau_e\right)^{1/2}$, where D_e and τ e are the carrier diffusion coefficient and lifetime, respectively. Recombination-stimulated surface generation of point defects and their diffusion to the bulk lead to the formation of a defect-enriched surface layer of thickness $l_d = \left(D_d \tau_d\right)^{1/2} < l_{dif}, l_{abs}$, where D_d is the defect diffusion coefficient, τ_d is the defect lifetime. The main outflow of the point defects are misfit dislocations formed in the film due to a difference in the lattice constants of the film and substrate. Let us assume that the density of threading dislocations (misfit dislocations) in the surface layer of the PbTe film is ρ (cm^{-2}), and the average distance between the lines of dislocations $l = \rho^{-1/2}$. Then the time of defect recombination $\tau_d = l^2 / D_d = 1/\rho D_d$ and the thickness of the defect-rich layer on the surface of the

film CdTe equals $l_d = \left(D_d \tau_d\right)^{1/2} = \rho^{-1/2}$. In the case of $\rho = 4\times10^{-10}$ cm^{-2}, the thickness of the defect-rich layer is $l_d = 5\times10^{-6}$ cm.

Under highly nonequilibrium conditions produced by laser irradiation (elevated temperature, mechanical stress, recombination-stimulated diffusion) the surface point defects have a high mobility. When the defect density exceeds a critical level, the surface layer becomes unstable, and the planar surface geometry results in a periodically bent configuration, with accumulations of interstitials and vacancies in hillocks and valleys, respectively (DD-surface instability) [16]. On the sample surface, this is accompanied by an increase in the amplitude $\zeta\left(\mathrm{r},\mathrm{t}\right)$ of the DD-structure, formed by a combination of DD-gratings: normal surface displacement gratings in time, $\zeta\left(\mathrm{r},\mathrm{t}\right) = \sum_{\mathrm{q}} \zeta_{\mathrm{q}} \exp\left(\mathrm{iqr} + \lambda_{\mathrm{q}}\mathrm{t}\right)$, coupled with surface defect concentration gratings, $\mathrm{N_d}\left(\mathrm{r},\mathrm{t}\right) = \sum_{\mathrm{q}} \mathrm{n_d}\left(\mathrm{q}\right) \exp\left(\mathrm{iqr} + \lambda_{\mathrm{q}}\mathrm{t}\right)$, where λ_{q} is the growth rate of the DD-grating, and the grating wave-vector q is parallel to the surface. ζ_{q} and $\mathrm{n_d}\left(\mathrm{q}\right)$ are the corresponding amplitudes in the DD-theory, a scale parameter which determines a characteristic DD-grating period and, hence (according to the DD-theory [16]), the nanoparticle size has a thickness of the defect-rich surface layer produced by laser irradiation, $\mathrm{h} = \mathrm{l_d}$. For high defect densities the growth rate of a DD-grating, $\lambda_{\mathrm{q}} = \lambda_{\mathrm{q}}\left(\Lambda\right)$, is a bimodal function of its period, $\Lambda = 2\pi/\mathrm{q}$. The bimodality $\lambda_{\mathrm{q}} = \lambda_{\mathrm{q}}\left(\Lambda\right)$ is a result of going beyond the usual Kirchhoff approximation [19] in the calculating of the bending deformation of the surface layer, produced for the first time in [16].

The nonlinear three-wave interaction of the DD-gratings on an isotropic surface results in DD-instability development on the semiconductor surface and leads to the formation of a hexagonal cellular seed DD-superstructure [17] in which the particle size distribution over L cells (nanoparticle nuclei) is governed by the bimodal growth rate $\lambda_{\mathrm{q}} = \lambda_{\mathrm{q}}\left(\Lambda\right)$ [16]. The formation of such hexagonal structure of the surface relief in the experiment is confirmed by the Fourier transform images of the irradiated surface (see [11]).

The spatially periodic defect distribution in a seed DD-structure leads to a spatially periodic modulation of the vaporisation rate of atoms on the semiconductor surface being irradiated by the laser beam: the vaporisation rate is higher in the valleys, which contain accumulations of vacancies, in comparison with the hillocks, which contain accumulations of interstitials. As a result, the sample surface irreversibly acquires a hexagonal cellular structure (of nanoparticles). The nanoparticle size distribution function then replicates the cell size distribution function in the seed DD-structure, which can be expressed through the bimodal growth rate $\lambda_{\mathrm{q}} = \lambda_{\mathrm{q}}\left(\Lambda\right)$ [16].

Fig. 5 compares the calculated nanoparticle size distribution function [16] to the experimental data (cf. 11).

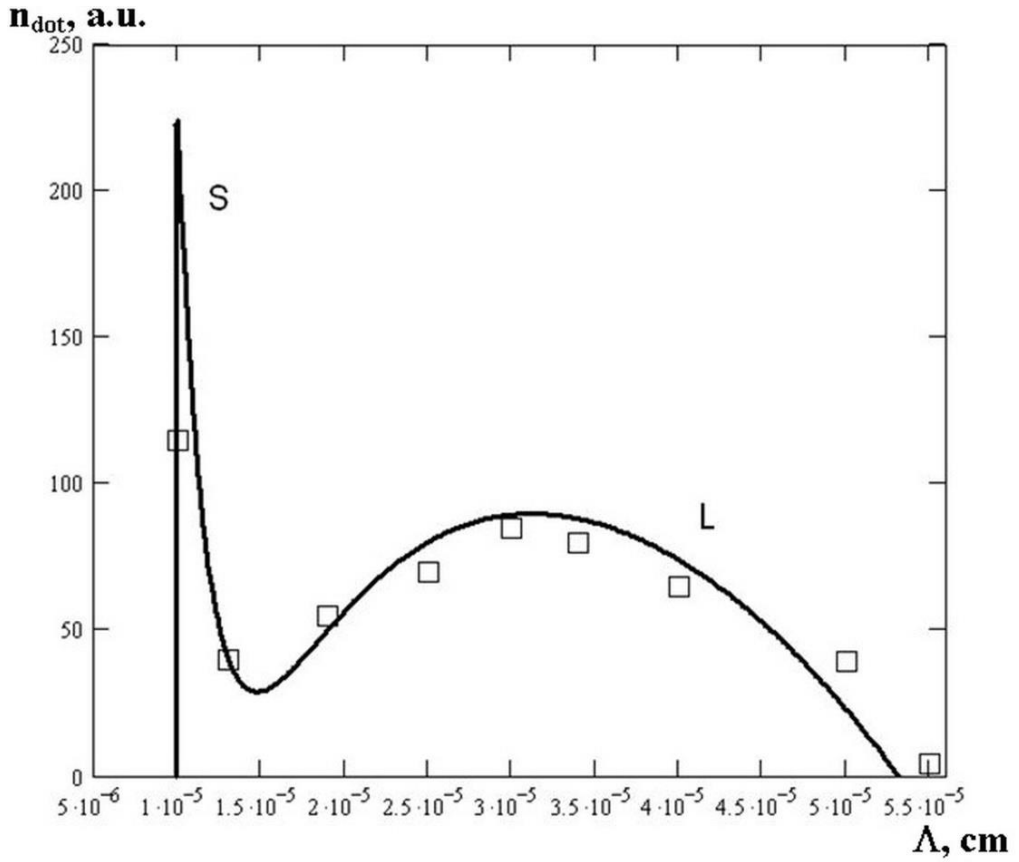

Fig. 5. Theoretical bimodal distribution function normalized by the lateral dimensions of the nanoparticles (solid line), calculated in [17] in comparison with the experimental dependence (squares) [11].

The theoretical curve fits with the histograms (Fig. 2) of the particle distribution under the laser beam irradiation. The calculated nanoparticle size distribution (Fig. 5) has two maxima at $\Lambda_c = 10^{-5}$ cm (S-peak) and $\Lambda_m = 3\times10^{-5}$ cm (L-peak), in agreement with the experimental data in Fig. 2. The curve adequately represents the experimentally determined distribution over the whole range of detected nanoparticle sizes.

The DD-theory also describes the linear dependence between the nanoparticle density and the laser intensity (see Fig. 3). The size of one cell of the hexagonal DD-superstructure according to [16] is equal to $2l_d$ (S-peak, Fig. 5). Because of that the quantity of cells (nanoparticle density) at the surface is $N = 1/4l_d = \rho/4$. The quantity of misfit dislocations $\rho = A\cdot\Delta a$, where A – a constant, Δa – the difference in the lattice constants for the film and the substrate [18]. Laser heating results in $\Delta a = \Delta\alpha_T \cdot \Delta T$, where $\Delta\alpha_T$ is the difference in thermal expansion coefficients of the film and the substrate, $\Delta T = BI$ is the change temperature of the film-substrate by laser heating, B – constant, I – intensity of laser radiation. The result is that the density of nanoparticles $N = const\cdot I$, which corresponds to the experimental linear dependence N on the laser intensity I (in Fig. 3).

Thus, the DD-theory [16] adequately describes the entire set of experimental data obtained by us (cf. [11]).

6. Classical diffusion model of the formation of a bimodal particle ensemble

For the comparison of DD-theory results and classical methods of modeling of forming clusters we have used the imitation model of moving and self-assembling processes crystal lattice defects. To describe the process of diffusion

of lattice defects during the process of laser heating for the model of moving atoms and vacancies the replacement algorithm was used. Vacancies which are formed on the surface of the sample had moved into the volume of the film during the heating process. The calculation area is a three dimensional cubic lattice with dimensions of 250x250x250 nodes, the distance between the nodes corresponded to the lattice constant PbTe - 6,46Å (the grid spacing k = 0,646 conventional units). Thus, in the actual size, the volume of 1 μm^3 was modeled. The diffusion coefficient of defects D_d is:

$$D_d = \frac{1}{6}\Delta^2 \Gamma , \tag{3}$$

where Δ − defect jump length (lattice constant), Γ − defect jump frequency in three-dimensional lattice. During laser heating then active formation of vacancies on the surface the diffusion coefficient of vacancies can reach to $D_d \approx 10^{-10}$ cm^2/s [20], that results in jump frequency $\Gamma \approx 10^8$ Hz and then average diffusion length $l_d = \sqrt{\Delta^2 \Gamma \tau} \approx 1$ μm (heating time τ = 1 s).

The reference center of laser heating was located in the upper left corner, the heating had took place over the entire height of the model volume of the substance. The new parameter was introduced: p - mobility coefficient, which could change from 0 to1, showing the difference between the diffusion coefficient near laser heating and the diffusion coefficient in lower layers of the material (distance from the laser focus in height). 100,000 particles (defects) (PbTe spherical molecules, lead and tellurium atoms with conventional dimensions 0.250, 0.175, 0.160) were introduced in the considered model volume. All of the particles made simultaneously chaotic motion over the lattice in the form of fractional Brownian motion (The "Ant" algorithm), on each step a particle have made a move in one of six neighbor nodes:

$$S_n + 1 = S_n + d_s , \tag{4}$$

where S is one of the axis S = [XYZ], coordinates about other axis remained the same. Change in the selected axis d_s = [-k 0 k]. As the particle was approached to the surface, the condition of nonnegative sampling was imposed on d_z.

There was assumed that at a meeting of any two particles larger one can absorb smaller, forming a spherical cluster. When cluster sizes were greater than lattice parameter of PbTe, the moving algorithm changes. Defects with dimensions which are greater than the lattice constant can't be tied to it, a new motion was introduced which can be described by the general laws of motion of particles in space.

When the cluster aggregation had consisted of more than 30 particles, it lost his mobility and became a germ aggregate. For the cluster with less quantity of particles - the jump frequency was recalculated. After contact of wandering particles with neighboring to the aggregate cells they were captured and became a part of the aggregate. The binding of each individual particle in the aggregate no new particle in the modeling space were added. The example of the defect migration during laser heating is shown in Fig. 6.

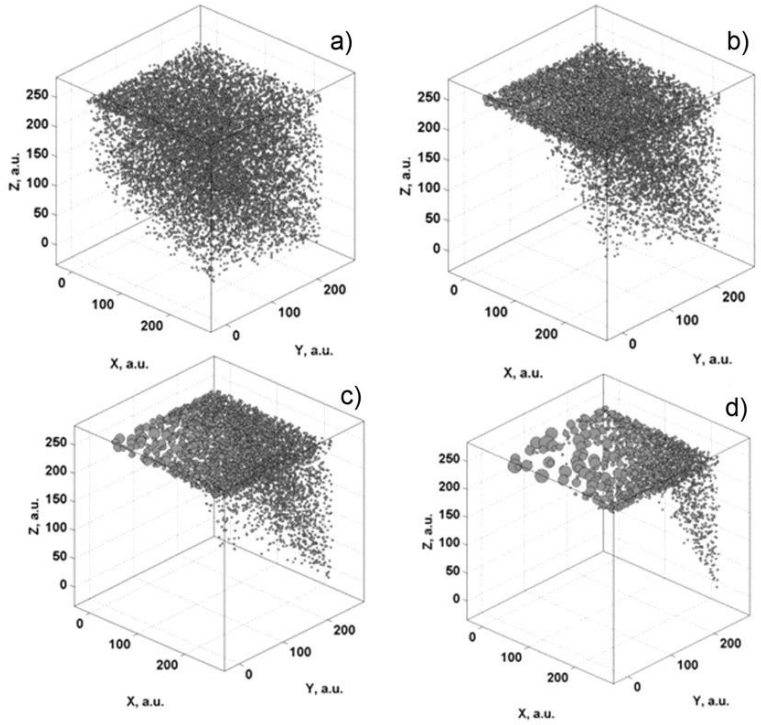

Fig. 6. The migration of particles and the formation of clusters in the model space in time: 0.2 s (a); 0.4 s (b); 0.6 s (c); 1 s (d).

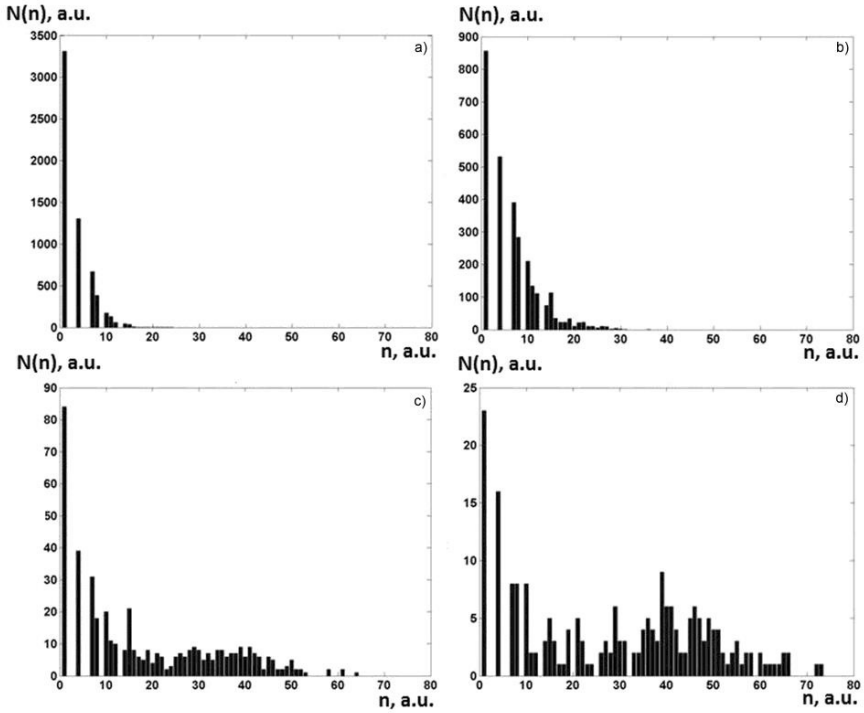

Fig. 7. Changing the distribution clusters histogram with n-particles in time: 0.2 s (a); 0.4 s (b); 0.6 s (c); 1 s (d).

The initial distribution of defects was uniform, during 0,2 s (Fig. 6.a) defects exited up to surface and clusters combined up to 15 molecules of PbTe (Fig. 6.a, 7.a) were formed. During 0,4 s atoms and molecules which were in the maximum heating area almost all of them had moved up to the surface and first critical germs were formed (Fig. 6.b, 7.b). After additional 0,2 s of laser radiation the clearly expressed area of surface modification was formed (Fig. 6.c, 7.c). The formation of the second peak in the area of clusters with larger sizes than critical germ was observed on the cluster size distribution histogram (Fig. 7.c).

The results of laser radiation of the surface of the modeling space is observed in the picture (Fig. 6.b, 7.b). This picture almost similar to experimental results in fig. 1 and 2. It is necessary to note that modeling experiments were calculated for different conditions (changing sizes of critical germ, coefficient of particle diffusion etc.), in this case results for most cases were similar, only the maxima intensity and histogram width were changeable. However, the relative positions of the maxima, require special consideration.

Conclusion

The experimental results of forming of nanoparticle ensemble with a bimodal distribution on the surface of the PbTe epitaxial films under the cw-laser modification are presented. The linear increase in the number of nanoparticles vs laser intensity in the range 10^5-10^6 W/cm^2 has been obtained. The changing of the distribution histograms of the particle diameter depending on the laser exposure has been experimentally studied. To describe the experimental results the defect-deformation (DD) theory of the formation of the ensemble of nanoparticles under CW-laser irradiation has been applied.

Finally, the effect of nanoparticle formation under the action of CW-laser radiation on a binary semiconductor allows to prepare the ensembles of semiconductor nanoparticles, in both simple and controlled method for future applications in electronics and photonics.

The authors thank Dr. H.Zogg (ETH, Zurich) for providing the epitaxial structures. Scientific publication is partly supported by government program number 16.440.2014/К; grants of Russian Foundation for Basic Research #13-02-97513 r_center_a, #13-02-00381_a, #14-02-97506 r_center_a, President grant for leader scientific school #89.2014.2; President grant for young PhD # 4321.2014.2.

References

1. Makarov G.N.Physics Uspekhi V.183,#7, pp. 673-720.
2. Efros Al. L., Efros A.L. Semiconductors 161209 (1982).
3. Brus L.E.J. Chem. Phys. 80 4403 (1984).
4. Chubilleau C., Lenoir B., Migot S., Dauscher A. Laser fragmentation in liquid medium: A new way for the synthesis of PbTe nanoparticles // Journal of Colloid and Interface Science 357 (2011) 13–17.
5. Joshua J. Choi et all. Controlling NanocrystalSuperlattice Symmetry and Shape-Anisotropic Interactions through Variable Ligand Surface Coverage// J. Am. Chem. Soc. 2011, 133, 3131–3138.
6. Feng Zhang et. All Laser Activation Modification of Semiconductor Surfaces (LAMSS) Langmuir, Vol. 22, No. 26, 2006 pp. 10859-10863.
7. Couillard M., Borowiec A., Haugen H.K., Preston J.S., Griswold E.M., Botton G.A., Subsurface modifications in indium phosphide induced by single and multiple femtosecond laser pulses: A study on the formation of periodic ripples// J Appl Phys vol. 101 (3) pp. 033519 (2007).
8. Shen M., Crouch C., J Carey, Younkin R., Mazur E. Formation of regular arrays of silicon microspikes by femtosecond laser irradiation through a mask// Appl. Phys. Lett. vol. 82 (11) (2003).
9. Shimotsuma Y., Sakakura M., Kanehira S., Qiu J., Kazansky P.G., Miura K., Fujita K., Hirao K. Three-dimensional Nanostructuring of Transparent Materials by the Femtosecond Laser Irradiation// Journal of Laser Micro/Nanoengineering," vol. 1 (3) 181 (2006).
10. Antipov A.A., Arakelian S.M., Zimin S.P., Kutrovskaya S.V., Kucherik A.O., OsipovA.V., Prokoshev V.G. Laser formation of semiconductor coatings using droplet technology// Physics Procedia 39 (2012) 401-408.
11. Antipov A.A., Arakelian S.M., Emel'yanov V.I., Zimin S.P., Kutrovskaya S.V., Kucherik A.O., Prokoshev V.G. Quantum electron 41(8), 735-737(2011).
12. Antipov A.A., Arakelian S.M., Emel'yanov V.I., Zimin S.P., Kutrovskaya S.V., Kucherik A.O., Prokoshev V.G. Quantum electron, 41(5), 441-446(2011).
13. Jianfei Wang, Juejun Hu, Xiaochen Sun, Anuradha M. Agarwa, Lionel C. Kimerling, Desmond R. Lim and R. A. Synowicki Structural, electrical, and optical properties of thermally evaporated nanocrystalline PbTe films// Journal of applied physics 104, 053707 (2008).
14. Zimin S.P., Gorlachev E.S., Amirov I.I., Gerke M.N., Zogg H., Zimin D. Role of threading dislocations during treatment of PbTe films in argon plasma // Semicond. Sci. Technol. – 2007. – Vol. 22, No. 8. – P. 929-932.

15. Gert-willem Räomer Matlab Laser Toolbox User Manual. http://www.utwente.nl/ctw/wa/software/laser/Matlab-Laser-Toolbox-User-Manual-0.1beta.pdf.
16. Emel'yanov V.I. Quantum electron, 41(8), 738-741 (2011).
17. Emel'yanov V.I. and Seval'nev D.M., Defect-Deformational Kuramoto–Sivashinsky Equation and Formation of Surface Nano- and Microstructures under the Laser and Ion-Beam Irradiation, Laser Physics,21, 566 (2011).
18. Landau L.D., Lifshitz E.M., Theory of Elasticity, Nauka, Moscow (1987).
19. Arsenault R. J., Shi N. Dislocation Generation Due to Differences between the Coefficients of Thermal Expansion// Materials Science and Engineering, 81, 175-187(1986).
20. R. J. Arsenault, N. Shi. Materials Science and Engineering. 81, (1986).